S©MR

СИБИРСКИЕ ЭЛЕКТРОННЫЕ
МАТЕМАТИЧЕСКИЕ ИЗВЕСТИЯ
Siberian Electronic Mathematical Reports
http://semr.math.nsc.ru
ISSN 1813-3304

Vol. 22, No. 2, pp. 1448–1472 (2025)
https://doi.org/10.33048/semi.2025.22.089

УДК 517.984.5, 532.135
MSC 35B35, 76A05, 76A10

LINEAR INSTABILITY OF A RESTING STATE FOR FLOWS OF POLYMERIC FLUID IN CYLINDER CHANNEL (VINOGRADOV-POKROVSKI MODEL)

D.L. TKACHEV, **E.A. BIBERDORF**

Communicated by O.S. Rozanova

Abstract: We study the linear stability of a resting state for flows of incompressible viscoelastic polymeric fluid in an infinite cylindrical channel in axisymmetric perturbation class. We use structurally-phenomenological Vinogradov-Pokrovski model as our mathematical model.

We state several analytically equivalent spectral problems: two for equation systems and another two for high-order equations we can get from them. Our numerical experiments show that with the growth of perturbations frequency along the channel axis there appear eigenvalues with positive real part. Moreover it turns out that one of the problems for the system gives more accurate results. That guarantees linear Lyapunov instability of the resting state.

Keywords: incompressible viscoelastic polymeric medium, rheological correlation, resting state, linearized mixed problem, Lyapunov stability.

Tkachev, D.L. Biberdorf E.A., Linear instability of a resting state for flows of polymeric fluid in cylinder channel (Vinogradov-Pokrovski model).

The study was carried out within the framework of the state contract of the Sobolev Institute of Mathematics (project no. FWNF-2022-0008).
Received November, 5, 2025, Published December, 29, 2025.

1 Introduction

To study the flows of an incompressible viscoelastic polymeric fluid in an infinite cylindrical channel we use structural-phenomenological Vinogradov-Pokrovski model as a base [1, 2]. This model interprets polymeric medium as a suspension of polymer macromolecules moving in an anysotropic fluid consisting of, e.g., solvent and other macromolecules. The environment effects on a chosen macromolecule is approximated by the impact on a chain of brownian particles, each of which is a sufficiently large part of the macromolecule. It turns out that the formulated physical model is an effective way of describing slow relaxation processes in mediums with linear polymers. In particular it is effective in numerical studies of polymer flows in areas with complex boundary geometry which are common for technological processes of making products from polymers.

Using a mechanical analogy we call the brownian particles "beads" and the analogue of the elastic powers between the particles "springs". In the simplest case when the macromolecule is modelled as a "dumbbell" ("dumbbell" is two beads connected by a spring), we formulate the system of differential correlations (Vinogradov-Pokrovski model):

$$\rho(\frac{\partial}{\partial t}v_i + v_l\frac{\partial}{\partial x_l}v_i) = \frac{\partial}{\partial x_k}\sigma_{il}, \quad \frac{\partial v_i}{\partial x_i} = 0, \tag{1}$$

$$\sigma_{il} = -p\delta_{il} + 3\frac{\eta_0}{\tau_0}a_{il}, \tag{2}$$

$$\frac{d}{dt}a_{il} - v_{ij}a_{jl} - v_{lj}a_{ji} + \frac{1+(k-\beta)I}{\tau_0}a_{il} = \frac{2}{3}\gamma_{il} - \frac{3\beta}{\tau_0}a_{ij}a_{jl}, \tag{3}$$

$$I = a_{11} + a_{22} + a_{33}, \quad \gamma_{il} = \frac{v_{il} + v_{li}}{2}, \quad i,l = 1,2,3. \tag{4}$$

Here ρ is polymer density, v_i is i-th velocity component, σ_{il} is stress tensor, p is pressure; η_0, τ_0 are initial values of shear viscosity and relaxation time for viscoelastic component, v_{il} is velocity gradient tensor ∇v, where it's components are calculated as follows: $v_{il} = \frac{\partial v_i}{\partial x_l}$, $i,l = 1,2,3$; γ_{il} is symmetrized velocity gradient tensor; a_{il} is symmetric anisotropy stress tensor; k and β are phenomenological parameters that take into account the size and the form of a macromolecule ball. Equations (1) are motion equation and incompressibility condition, and equations (2)-(3) are rheological correlation, that connects kinematic characteristics of the flow with its thermodynamic parameters; for each component a_{il} the sum of the first three terms in the left part of equality (3) is the so called upper convective derivative or Oldroyd derivative [3], $\frac{d}{dt} = \frac{\partial}{\partial t} + (\vec{v}, \nabla)$ is material derivative.

Note that the accepted physical representation of a polymeric medium allows us to describe its main rheological properties: the decrease of viscosity and the first difference of normal stresses with the growth of shear velocity, the growth of stretching viscosity to a certain limit with the growth of deformation velocity.

Moreover, unlike the known models FENE-R [4], FENE-CR [5] that take into account additional physical mechanisms reflecting the behaviour features of a studied material: boundedness and nonlinearity of a spring elongation, connected to the finite length of a macromolecule and the existence of weaves and engagements in it, which obstruct its uniform and infinite elongation (instead of a Hooke law the nonlinear law of a spring elasticity is used); or RHL-model [6] that takes into account potential barriers, that slow down the transition from one equilibrium configuration to the other (additional force of an inner resistance is introduced), the Pokrovski-Vinogradov model allows us to acquire nonzero values of the second difference for normal stresses. Specifically, it tries to take into account the anisotropy effect of the chosen molecule environment that is caused by its elongation and orientation in space during the flow process of its macromolecule chains.

Rheological properties, predicted by the Pokrovski-Vinogradov model with parameters $k = 1, 2\beta$, that guarantee monotone of a flow curve, are qualitatively and quantitatively agree with the experimental data for melts and solutions of polymers [7, 8, 9].

A number of previous works by one of the authors [10, 11] studied the linear Lyapunov stability of Poiseuille-type flows in an infinite plane channel (the pressure drop on a segment doesn't depend on time) for the model (1)-(4), as well as for its generalization on the case of nonisothermic flow of an incompressible weakly conducting polymeric fluid with the existence of a negative space charge [12, 13, 14, 15] and on the case of nonisothermic model with the additional external interaction of a uniform magnetic field [16, 17, 18, 19].

In particular, in work [10] it was proven that the Poiseuille-type flow for the model (1)-(4) is linearly unstable in a perturbation class of generalized functions from the Schwartz space S' of the functions of slow growth with respect to the x variable, that changes along the channel side [20, 21]. I.e. the solution of a linearized problem is growing as an exponential function with the power st, $s = i\xi\hat{u} + \sqrt[3]{Q(y)}\xi^{\frac{2}{3}} + o(\xi^{\frac{2}{3}})$, for $|\xi| \to \infty$ (ξ is a dual variable for variable x with respect to the Fourier transform, $\hat{u}$ is a component of the base Poiseuille-type flow, $Q(y) \neq 0$, is a function, that depends on the problem parameters and its base solution, "o" is small o).

The question of stability of the resting state for nonisothermic model of the polymeric fluid flow in an infinite plane channel under the influence of an external magnetic field was studied in works [22, 23, 24]. The main result being that the resting state in the case of an absolute conductivity, i.e. vanishing of the parameter inversly proportional to the magnetic Reynolds number, and additionally vanishing of one of the dissipative coefficients is linearly unstable by Lyapunov. The conducting walls of the channel can be made from different materials: ebonite, aluminum, copper, platinum, bismuth.

For the analysis of the applicability of mathematical models for the description of real flows of polymeric fluid of special interest is the question about

the stability of the resting state of the model. From the physical point of view this property is a necessary one.

The result of the work [25] was refined in the works [26, 27]. It states that the spectrum of a linearized with respect to the resting state mixed problem for the system (1)–(4) does not lie in an open right half-plane. One of the main results of these works is that the mixed problem has solutions with more than exponential growth $e^{Re\lambda t}$, $Re\lambda > 0$, $t \to +\infty$.

Which means that the resting state for plane-parallel flows of polymeric fluid in the Vinogradov-Pokrovski model is linearly unstable by Lyapunov.

In the current work we continue to study the location of the spectrum of a linear problem about the flow of a polymeric fluid in an infinite cylindrical channel. As a base solution we again chose the resting state and as a perturbation class we choose perturbations with axial symmetry and periodic with respect to the variable varying along the channel axis.

Note that the study of the flows of fluids of different nature in domains with cylindrical boundaries is fundamentally important not only from the point of view of a boundary geometry influencing the formation of characteristic features of the flow (alike the flows of viscous fluid (Navier-Stokes model) between the two coaxial rotating cylinders in the classic Taylor work [28]), but also to have the ability to experimentally check the picture of a flow predicted by the model.

We got a number of results in [29] both for small values of parameters Wi and Re, e.g. $Wi = 1.1 \cdot 10^{-6}$, $Re = 10^{-2}$, and for large ones, e.g. $Wi = 3 \cdot 10^{3}$, $Re = 5 \cdot 10^{3}$. In our numerical experiments for some values of n, i.e. spacial frequency of perturbations, part of the spectrum lies in an open right half-plane but with its growth there can be a sharp increase of the maximum values of real parts of eigenvalues. This experiments were done for the spectral problem for one longitudinal component of velocity. We got this problem after transforming the initial spectral problem for the system where boundary conditions are replaced with one asymptotic one.

Further we used the idea of reducing the spectral problem for the system into the problem for only the radial component of the velocity in [30, 31, 32, 33], which study the linearized with respect to the resting state mixed problem for flows of polymers in cylindrical channel under the effect of an external uniform magnetic field both for the case of absolute conductivity and in general case.

Of note is also the work [34] about the influence of the coefficient in the representation of the pressure drop (it depends on time) and the boundary condition for the temperature (the work considers nonisothermic case) on the stability of a Poiseuille-type solution for flows of polymeric fluid in a cylindrical channel.

In this work we continue the numerical study of spectral problems (38), (39) and their analogues. They differ in a way they approximate boundary conditions on the cylinder axis $r = 0$. We show that with the growth of parameter n (the frequency of perturbations) part of the spectrum transits

into the right half-plane which means linear instability of a resting state. The results from studying the spectral problem for the original system statement gives in our opinion a more reliable result.

2 Quasilinear and linearized models. Formulation of the main results

Following the monographs [1, 2, 36, 37, 38] and works [30, 31], we formulate the mathematical model for describing flows of an incompressible polymeric fluid in an infinite cylinder channel with round section (see Fig. 1).

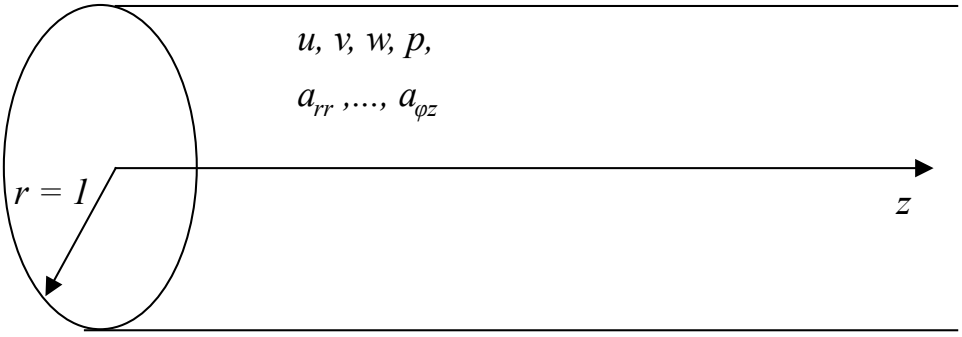

FIGURE 1. Cylindrical channel and main parameters of the polymeric fluid flow

We can write the model in a dimensionless form and in a cylindrical coordinate system as follows:

$$div\mathbf{u} = \frac{1}{r}\frac{\partial(ru)}{\partial r} + \frac{1}{r}\frac{\partial v}{\partial \varphi} + \frac{\partial w}{\partial z} = 0, \tag{5}$$

$$\frac{du}{dt} - \frac{v^2}{r} + \frac{\partial p}{\partial r} = \frac{1}{Re}\left(\frac{\partial a_{rr}}{\partial r} + \frac{1}{r}\frac{\partial a_{r\varphi}}{\partial \varphi} + \frac{\partial a_{rz}}{\partial z} + \frac{a_{rr} - a_{\varphi\varphi}}{r}\right), \tag{6}$$

$$\frac{dv}{dt} + \frac{uv}{r} + \frac{1}{r}\frac{\partial p}{\partial \varphi} = \frac{1}{Re}\left(\frac{\partial a_{r\varphi}}{\partial r} + \frac{1}{r}\frac{\partial a_{\varphi\varphi}}{\partial \varphi} + \frac{\partial a_{\varphi z}}{\partial z} + \frac{2a_{r\varphi}}{r}\right), \tag{7}$$

$$\frac{dw}{dt} + \frac{\partial p}{\partial z} = \frac{1}{Re}\left(\frac{\partial a_{rz}}{\partial r} + \frac{1}{r}\frac{\partial a_{\varphi z}}{\partial \varphi} + \frac{\partial a_{zz}}{\partial z} + \frac{a_{rz}}{r}\right), \tag{8}$$

$$\frac{da_{rr}}{dt} - 2\left(A_r\frac{\partial u}{\partial r} + \frac{a_{r\varphi}}{r}\frac{\partial u}{\partial \varphi} + a_{rz}\frac{\partial u}{\partial z}\right) + L_{rr} = 0, \tag{9}$$

$$\frac{da_{\varphi\varphi}}{dt} + 2\left(\frac{v}{r} - \frac{\partial v}{\partial r}\right)a_{r\varphi} - 2\left(\frac{1}{r}(u + \frac{\partial v}{\partial \varphi})A_\varphi + a_{\varphi z}\frac{\partial v}{\partial z}\right) + L_{\varphi\varphi} = 0, \tag{10}$$

$$\frac{da_{zz}}{dt} - 2\left(a_{rz}\frac{\partial w}{\partial r} + \frac{a_{\varphi z}}{r}\frac{\partial w}{\partial \varphi} + A_z\frac{\partial u}{\partial z}\right) + L_{zz} = 0, \tag{11}$$

$$\frac{da_{r\varphi}}{dt}+\left(\frac{v}{r}-\frac{\partial v}{\partial r}\right)A_r+\left(a_{r\varphi}\frac{\partial w}{\partial z}-a_{rz}\frac{\partial v}{\partial z}-\frac{A_\varphi}{r}\frac{\partial u}{\partial \varphi}-a_{\varphi z}\frac{\partial u}{\partial z}\right)+L_{r\varphi}=0, \tag{12}$$

$$\frac{da_{rz}}{dt}-a_{rz}\left(\frac{\partial u}{\partial r}+\frac{\partial w}{\partial z}\right)-\left(A_r\frac{\partial w}{\partial r}+\frac{a_{r\varphi}}{r}\frac{\partial w}{\partial \varphi}+\frac{a_{\varphi z}}{r}\frac{\partial u}{\partial \varphi}+A_z\frac{\partial u}{\partial z}\right)+L_{rz}=0, \tag{13}$$

$$\frac{da_{\varphi z}}{dt}+\left(\frac{v}{r}-\frac{\partial v}{\partial r}\right)a_{rz}-\left(a_{\varphi z}\frac{\partial u}{\partial r}+A_z\frac{\partial v}{\partial z}+a_{r\varphi}\frac{\partial w}{\partial r}+\frac{A_\varphi}{r}\frac{\partial w}{\partial \varphi}\right)+L_{\varphi z}=0. \tag{14}$$

In equations (5)–(14) t is time, u, v, w are components of a velocity vector $\mathbf{u}$ in a cylindrical coordinate system; p is hydrodynamic pressure; $a_{rr}, \ldots, a_{\varphi z}$ are components of a symmetrical anisotropy tensor Π of a second rank [1, 2];

$$L_{rr}=K_I a_{rr}+\beta\|a_r\|^2,\quad L_{\varphi\varphi}=K_I a_{\varphi\varphi}+\beta\|a_\varphi\|^2,\quad L_{zz}=K_I a_{zz}+\beta\|a_z\|^2,$$
$$L_{r\varphi}=K_I a_{r\varphi}+\beta(a_r,a_\varphi),\ L_{rz}=K_I a_{rz}+\beta(a_r,a_z),\ L_{\varphi z}=K_I a_{\varphi z}+\beta(a_\varphi,a_z),$$
$$a_r=(a_{rr},a_{r\varphi},a_{rz}),\quad a_\varphi=(a_{r\varphi},a_{\varphi\varphi},a_{\varphi z}),\quad a_z=(a_{rz},a_{\varphi z},a_{zz}),$$
$$A_r=a_{rr}+Wi^{-1},\quad A_\varphi=a_{\varphi\varphi}+Wi^{-1},\quad A_z=a_{zz}+Wi^{-1},$$
$$K_I=Wi^{-1}+\bar{k}I/\beta,\quad I=a_{rr}+a_{\varphi\varphi}+a_{zz},\quad \bar{k}=k-\beta,$$

the square of the vector norm $\|\cdot\|^2$ is the sum of squares of its components, k, β, $0<\beta<1$ are phenomenological parameters of a rheological model [1, 2], $Re=(\rho u_H l)/\eta_0$ is the Reynolds number, $Wi=(\tau_0 u_H)/l$ is the Weissenberg number, $\rho(=const)$ is the density of the medium, η_0, τ_0 are initial values of shear viscosity and relaxation time [1, 2], l is the characteristic length, u_H is the characteristic velocity, $\triangle_{r,\varphi,z}=\frac{\partial^2}{\partial r^2}+\frac{1}{r^2}\frac{\partial^2}{\partial \varphi^2}+\frac{1}{r}\frac{\partial}{\partial r}+\frac{\partial^2}{\partial z^2}$ is the Laplace operator, $\frac{d}{dt}=\frac{\partial}{\partial t}+u\frac{\partial}{\partial r}+\frac{v}{r}\frac{\partial}{\partial \varphi}+w\frac{\partial}{\partial z}$.

The system (5)–(14) is written in a dimensionless form: variables t, r, z, u, v, w, p, $a_{rr}, \ldots, a_{\varphi z}$ are related to $l/u_H, l, u_H, \rho u_H^2, \frac{Wi}{3}$ correspondingly.

We state that the no-slip condition holds on the boundary $r=1$

$$\mathbf{u}=0, \tag{15}$$

and on the cylinder axis, i.e. for $r=0$, there are boundedness conditions on all the unknown variables $u, v, w, p, \alpha_{rr}, \ldots, \alpha_{\varphi z}$.

As a base solution we choose the resting state

$$\mathbf{u}=0,\quad p=p_0-const,\quad \alpha_{rr}=0,\ \ldots,\ \alpha_{r\varphi}=0.$$

Linearizing the boundary problem (5)–(15) with respect to the chosen solution results in a following problem (small perturbations of the components of the solution are written the same as initial variables)

$$Ru+\frac{1}{r}v_\varphi+w_z=0, \tag{16}$$

$$u_t + \Omega_r = \frac{1}{r}(\alpha_{r\varphi})_\varphi + (\alpha_{rz})_z + \frac{\alpha_{rr} - \alpha_{\varphi\varphi}}{r}, \tag{17}$$

$$v_t + \frac{1}{r}\Omega_\varphi = (\alpha_{r\varphi})_r + \frac{1}{r}(\alpha_{\varphi\varphi} - \alpha_{rr})_\varphi + (\alpha_{\varphi z})_z + \frac{2\alpha_{r\varphi}}{r}, \tag{18}$$

$$w_t + \Omega_z = (\alpha_{rz})_r + \frac{1}{r}(\alpha_{\varphi z})_\varphi + (\alpha_{zz} - \alpha_{rr})_z + \frac{\alpha_{rz}}{r}, \tag{19}$$

$$\Lambda\alpha_{rr} = 2\varkappa^2 u_r, \tag{20}$$

$$\Lambda\alpha_{\varphi\varphi} = \frac{2}{r}(u + v_\varphi)\varkappa^2, \tag{21}$$

$$\Lambda\alpha_{zz} = 2\varkappa^2 u_z, \tag{22}$$

$$\Lambda\alpha_{r\varphi} = \frac{\varkappa^2}{r}u_\varphi - \varkappa^2\left(\frac{v}{r} - v_r\right) \tag{23}$$

$$\Lambda\alpha_{rz} = \varkappa^2(w_r + u_z), \tag{24}$$

$$\Lambda\alpha_{\varphi z} = \varkappa^2(v_z + \frac{w_\varphi}{r}). \tag{25}$$

$$u = 0, \quad \text{for } r = 1.$$

Here $\alpha_{rr} = \frac{a_{rr}}{Re}, \ldots, \alpha_{\varphi z} = \frac{a_{\varphi z}}{Re}$, $\varkappa^2 = \frac{1}{WiRe}$, $R = \frac{\partial}{\partial r} + \frac{1}{r}$, $\Lambda = \frac{\partial}{\partial t} + \frac{1}{Wi}$, $\Omega = p - \alpha_{rr}$.

Remark 1. *For the function Ω, i.e. generalized "pressure", the following correlation holds*

$$D_0\Omega = \left(\frac{1}{r^2}\frac{\partial^2}{\partial\varphi^2} - \frac{1}{r}\frac{\partial}{\partial r}\right)(\alpha_{\varphi\varphi} - \alpha_{rr}) + \\ + 2R\left(\frac{\partial}{\partial z}\alpha_{rz} + \frac{1}{r}\frac{\partial}{\partial\varphi}\alpha_{r\varphi} + \frac{2}{r}\frac{\partial}{\partial\varphi}\left(\frac{\partial}{\partial z}\alpha_{\varphi z} + \frac{1}{r}\alpha_{r\varphi}\right)\right), \tag{26}$$

where $D_0 = \triangle = \frac{\partial^2}{\partial r^2} + \frac{1}{r}\frac{\partial}{\partial r} + \frac{1}{r^2}\frac{\partial^2}{\partial\varphi^2} + \frac{\partial^2}{\partial z^2} = R^2 + \frac{1}{r^2}\frac{\partial^2}{\partial\varphi^2} + \frac{\partial^2}{\partial z^2}$.

We will be looking for a solution of the problem (16)–(25) in the special form:

$$u(t, r, \varphi, z) = u(r)\exp\{\lambda t + inz + im\varphi\}, \ldots, \\ \alpha_{\varphi z}(t, r, \varphi, z) = \alpha_{\varphi z}(r)\exp\{\lambda t + inz + im\varphi\}, \tag{27}$$

where $\lambda = \eta + i\xi$, $\xi, \eta \in R^1$, $n, m \in Z$ are some parameters.

Then for the components of the anisotropy tensor under the additional condition

$$\lambda \neq -\frac{1}{Wi} \tag{28}$$

we get the following:

$$\begin{cases} \alpha_{rr} = \dfrac{u'}{\hat{\lambda}}, \quad \alpha_{\varphi\varphi} = \dfrac{u + imv}{r\hat{\lambda}}, \quad \alpha_{zz} = \dfrac{inu}{\hat{\lambda}}, \\ \alpha_{r\varphi} = \dfrac{1}{2\hat{\lambda}} \left\{ \dfrac{imu}{r} + v' - \dfrac{v}{r} \right\}, \quad \alpha_{rz} = \dfrac{w' + inu}{2\hat{\lambda}}, \\ \alpha_{\varphi z} = \dfrac{i(nv + \frac{1}{r}mw)}{2\hat{\lambda}}, \quad \hat{\lambda} = \dfrac{\lambda + Wi^{-1}}{2\varkappa^2}. \end{cases} \tag{29}$$

The other four equations of the system (16)–(25) are rewritten as follows:

$$Ru + i(\frac{m}{r}v + nw) = 0, \tag{30}$$

$$\Omega' = -\left(\frac{m^2 + 2}{2r^2\hat{\lambda}} + \frac{n^2}{2\hat{\lambda}} + \lambda \right) u + \frac{1}{r\hat{\lambda}}u' + \frac{im}{2\hat{\lambda}r}(v' - \frac{3v}{r}) + \frac{in}{2\hat{\lambda}}w', \tag{31}$$

$$R^2 v - \left(n^2 + \frac{1 + 3m^2}{r^2} + 2\lambda\hat{\lambda} \right) v = \frac{2nm}{r}w - \frac{4im}{r^2}u + \frac{2im\hat{\lambda}}{r}\Omega, \tag{32}$$

$$R^2 w - \left(n^2 + \frac{m^2}{r^2} + 2\lambda\hat{\lambda} \right) w = 2in\hat{\lambda}\Omega + 2mnv + 2n^2 u - \frac{2inu}{r}. \tag{33}$$

From (17), (26) and (29) it follows that

$$\begin{aligned} d_0\Omega = &\left(-\frac{m^2}{r^2} - \frac{1}{r}\frac{d}{dr} \right) \left(\frac{u + imv}{r\hat{\lambda}} - \frac{u'}{\hat{\lambda}} \right) + \\ &+ R\left(in\frac{w' + inu}{\hat{\lambda}} + \frac{im}{r}\frac{\frac{imu}{r} + v' - \frac{v}{r}}{\hat{\lambda}} \right) + \\ &+ \frac{im}{r}\left(-n\frac{nv + \frac{1}{r}mw}{\hat{\lambda}} + \frac{1}{r}\frac{\frac{imu}{r} + v' - \frac{v}{r}}{\hat{\lambda}} \right) - n^2\left(\frac{inu}{\hat{\lambda}} - \frac{u'}{\hat{\lambda}} \right), \end{aligned} \tag{34}$$

$$\widetilde{\Omega}' = \frac{imv'}{2\hat{\lambda}} - \frac{inw'}{2\hat{\lambda}} \quad \text{for } r = 1, \tag{35}$$

where

$$\widetilde{\Omega} = \Omega - \frac{u}{r\hat{\lambda}} - \frac{in}{\hat{\lambda}}w. \tag{36}$$

Here

$$d_1 = d_0 - \frac{1}{r^2}, \quad d_0 = \frac{d^2}{dr^2} + \frac{1}{r}\frac{d}{dr} - \frac{m^2}{r^2} - n^2 = R^2 - \frac{m^2}{r^2} - n^2.$$

In an axisymmetric case, when $m = 0$, which is the main interest to us, the system (30)–(33) is simplified by splitting into two independent subsystems. That and the boundary conditions (25) leads us to the following two spectral boundary problems:

$$\begin{cases} (d_1 - 2\lambda\hat{\lambda})v = 0, \\ v = 0 \quad \text{for } r = 1, \\ |v(0)| < \infty; \end{cases} \tag{37}$$

$$\begin{cases} Ru + inw = 0, \\ (d_0 - 2\lambda\hat{\lambda})w - 2in\hat{\lambda}\check{\Omega} - 2n^2u + n^2w = 0, \\ \check{\Omega}' + \dfrac{2\lambda\hat{\lambda} + n^2}{2\hat{\lambda}}u = 0, \\ u = w = 0 \quad \text{for } r = 1, \\ |u(0)| < \infty, \quad |w(0)| < \infty. \end{cases} \tag{38}$$

Here

$$d_1 = R^2 - n^2 - \frac{1}{r^2}, \quad d_0 = R^2 - n^2, \quad \check{\Omega} = \widetilde{\Omega} + \frac{in}{2\hat{\lambda}}w,$$

function $\widetilde{\Omega}$ can be represented through Ω due to (35). The correlation (34) takes the following form:

$$d_0\widetilde{\Omega} = \frac{in^3}{\hat{\lambda}}(w - u).$$

Assume the parameter n is non-zero. Then by differentiating the second equation from the system (38) and replacing $\check{\Omega}'$ by using the third equation from the system (38) we can also replace w using the first equation and get to the spectral problem for one component u:

$$\begin{cases} u^{IV} + \dfrac{2}{r}u''' + u''\left(-\dfrac{3}{r^2} - 2\lambda\hat{\lambda}\right) + u'\left(\dfrac{3}{r^3} - \dfrac{2\lambda\hat{\lambda}}{r} + 2in^3\right) + \\ + u\left(-\dfrac{3}{r^4} + \dfrac{2\lambda\hat{\lambda}}{r^2} + n^2(2\lambda\hat{\lambda} + n^2)\right) = 0, \\ |u(0)| < \infty, \quad \left|(u' + \dfrac{1}{r}u)\big|_{r=0}\right| < \infty, \\ u(1) = 0, \quad u'(1) + u(1) = 0. \end{cases} \tag{39}$$

Remark 2. *The transition from the spectral problem (38) to the spectral problem (39) is the main idea of work [29]. It also studied the special cases where $\lambda = -\frac{1}{Wi}$, $n = 0$. There the spectrum points lie in a left complex half-plane $Re\lambda \le -\sigma < 0$ but can have multiplicity greater than one.*

In [29] we have proven the following theorem.

Theorem 1. *Let $\lambda \neq -\frac{1}{Wi}$. Then the spectral equation for the eigenvalues of the boundary problem (39) has the following form*

$$u_2'(1)u_1(1) - u_1'(1)u_2(1) = 0,$$

the functions $u_1(r)$ and $u_2(r)$ are defined through recurrent formulas

$$u_1 = \sum_{k=0}^{\infty} a_k r^{k+3} = a_0 r^3 + a_1 r^4 + a_2 r^5 + \dots, \tag{40}$$

$$\begin{gathered} a_0 = 1, \quad a_1 = 0, \quad a_2 = \frac{1}{24}\lambda\hat{\lambda}, \quad a_3 = -\frac{2}{175} i n^3, \\ a_k = \frac{2\lambda\hat{\lambda}}{(k+2)(k+4)} a_{k-2} - \frac{2in^3}{(k+2)^2(k+4)} a_{k-3} - \\ - \frac{n^2(2\lambda\hat{\lambda}+n^2)}{k(k+2)^2(k+4)} a_{k-4}, \; k = 4,5,6,\dots; \end{gathered} \tag{41}$$

$$u_2 = \sum_{k=0}^{\infty} c_k r^{k+1} = c_0 r + c_1 r^2 + c_2 r^3 + \dots, \tag{42}$$

$$\begin{gathered} c_0 = 1, \quad c_1 = 0, \quad c_2 = 0, \quad c_3 = -\frac{2}{45} i n^3, \\ c_k = \frac{2\lambda\hat{\lambda}}{k(k+2)} c_{k+2} - \frac{2in^3}{k^2(k-2)} c_{k-3} - \frac{n^2(2\lambda\hat{\lambda}+n^2)}{k^2(k-2)(k+2)} c_{k-4}, \; k = 4,5,6\dots \end{gathered} \tag{43}$$

In its turn the solution to the spectral problem (37) can be found in an explicit way:

$$v = J_1(i\sqrt{2\lambda\hat{\lambda}}r),$$

$$\lambda_{1,2} = \frac{-\frac{1}{Wi} \pm \sqrt{\frac{1}{Wi^2} - 4\varkappa^2(\mu_k^2 + n^2)}}{2},$$

where $J_1(\mu_k) = 0$, and $J_1(\xi)$ is a Bessel function of the first kind [35].

Remark 3. *Obviously* $Re\lambda_{1,2} \le -\sigma_1 < 0$.

3 Clarified spectral problems (38), (39) and their discretization

Denoting $\hat{\Omega} = 2\hat{\lambda}\check{\Omega}$ and $\mu = 2\lambda\hat{\lambda}$ the system from the spectral problem (38) can be rewritten as

$$\begin{cases} u' = -\dfrac{1}{r}u - inw, \\ w'' = -\dfrac{1}{r}w' + \mu w + in\hat{\Omega} + 2n^2 u, \\ \hat{\Omega}' = -(\mu + n^2)u, \end{cases} \tag{44}$$

linear with respect to the new spectral parameter μ.

Making the following variables change $\tilde{u} = ru$, $\tilde{w} = rw$, gives us system

$$\begin{cases} \tilde{u}' = -in\tilde{w}, \\ \tilde{w}'' = \dfrac{1}{r}\tilde{w}' + \left(\mu - \dfrac{1}{r^2}\right)\tilde{w} + inr\hat{\Omega} + 2n^2\tilde{u}, \\ r\hat{\Omega}' = -(\mu + n^2)\tilde{u}. \end{cases} \tag{45}$$

Elimination of variables leads to equations

$$u^{IV} + \frac{2}{r}u''' + u''\left(-\frac{3}{r^2} - \mu\right) + u'\left(\frac{3}{r^3} - \frac{\mu}{r} + 2in^3\right) + \\ + u\left(-\frac{3}{r^4} + \frac{\mu}{r^2} + n^2(\mu + n^2)\right) = 0, \tag{46}$$

$$\tilde{u}^{IV} - \frac{2}{r}\tilde{u}''' + \tilde{u}''\left(\frac{3}{r^2} - \mu\right) + \tilde{u}'\left(-\frac{3}{r^3} + \frac{\mu}{r} + 2in^3\right) + \\ + \tilde{u}\left(n^2(n^2 + \mu) - \frac{2in^3}{r}\right) = 0. \tag{47}$$

Systems and equations need to be completed by boundary conditions. On the cylinder surface ($r = 1$) we set the non-slip conditions:

$$u(1) = w(1) = 0, \tag{48}$$

which together with the first equation from system (44) also gives us

$$u'(1) = 0. \tag{49}$$

On the cylinder axis ($r = 0$) the most general would be the boundedness condition

$$|u(0)| < \infty, \qquad |w(0)| < \infty \tag{50}$$

and correspondingly

$$|u'(0)| < \infty. \tag{51}$$

These conditions were used in [29].

From the construction of the functions $\tilde{u}$, $\tilde{w}$ it follows that:

$$\tilde{u}(1) = \tilde{u}'(1) = \tilde{w}(1) = 0, \tag{52}$$

$$\tilde{u}(0) = u'(0) = \tilde{w}(0) = 0. \tag{53}$$

Theoretically speaking these conditions are enough to state spectral problems. But in case of systems we can add conditions on function $\hat{\Omega}$:

$$|\hat{\Omega}(0)| < \infty, \qquad |\hat{\Omega}(1)| < \infty. \tag{54}$$

From a mathematical point of view these conditions are excessive but from the physics point of view are rather natural. Adding these conditions does not lead to overdefinition of problems (44), (45) since solutions have to satisfy them anyways.

We are studying formulated above problems numerically. Note that in literature there are examples where using different discretization methods led to spectrum of very different structure (see e.g. [40]). Besides, the

discretization can lead to appearance of eigenvalues that do not converge to spectral points of differentiation operator with the growth of the dimensions of discrete approximation. Usually such "parasitic" eigenvalues correspond to saw-like eigenfunctions.

To discretize the problem we will use pseudospectral method with collocation nodes at points

$$r_j = \frac{\xi_j + 1}{2},$$

where $\xi_j = \cos\frac{\pi(N-j)}{N}$, $j = 0, 1, \ldots, N$, are Gauss-Lobatto points. We will denote a collocation matrix as $D \approx \dfrac{d}{dr}$ (see. [39]).

$$D = \begin{pmatrix} d_{00} & d_{01} & \ldots & d_{0\,N} \\ d_{10} & d_{11} & \ldots & d_{1\,N} \\ \vdots & \vdots & \ddots & \vdots \\ d_{N0} & d_{N1} & \ldots & d_{NN} \end{pmatrix}.$$

Mapping boundary conditions to the structure of collocation matrices derivatives is an important element of stating the discrete spectral problem. The easiest one is the homogeneous Dirichlet condition. To count it in we delete corresponding columns from the matrix (if further calculations allow for rectangular matrices) or simultaneously rows and columns (see [29], [39]). Below we will denote the collocation matrix derivative that satisfies Dirichlet condition for $r = 0$ and $r = 1$ as D^0 and D_0 correspondingly. If the function satisfies Dirichlet condition on both boundaries, we will denote it D_0^0.

One of the possible approaches to mapping other boundary conditions is to reduce them to Dirichlet condition. For example a function satisfying dual Dirichlet-Neumann condition $u(0) = u'(0) = 0$ has a form $u(r) = r \cdot v(r)$, where $v(0) = 0$. Hence, $u' = v + rv'$, which gives us expression for the corresponding matrix derivative: $D^{00} = (I + \mathrm{diag}(r_j)D^0)\mathrm{diag}\left(\frac{1}{r_j}\right)$, where I is a unity matrix (see [29], [39] and other works).

By analogy to this approach we can represent a bounded function $|u(0)| < \infty$ as a product $u(r) = \frac{1}{r} \cdot v(r)$, where $v(0) = 0$. Then the derivative is $u' = -\frac{1}{r^2}v + \frac{1}{r}v'$ and it's discrete representation is $D^{<\infty} = \mathrm{diag}\left(\frac{1}{r_j}\right)(-I + D^0\mathrm{diag}(r_j))$. We will call this approach a method of function multiplication. It was already used earlier in [32, 33].

To map conditions such as boundedness of eigenfunctions of the spectral problem we can also use asymptotic method (see [29, 32, 33]). Its essence is as follows. We write equation as

$$(L_1 - \mu L_2)u = 0, \qquad 0 \le r \le 1,$$

where $L_j(r, d/dr)$ are linear differential operators and eigenfunctions of the equation satisfy conditions

$$|u(0)| < \infty,\ |u'(0)| < \infty, \qquad u(1) = u'(1) = 0.$$

We assume that the function $u_0(r)$, which is an asymptotic of eigenfunctions in zero, is known

$$\lim_{r\to 0} \frac{u(r)}{u_0(r)} = 1,$$

and satisfies equation

$$(L_3 - \mu L_4)u_0 = 0, \qquad 0 \le r \le 1.$$

For example, for equation (46) operators $L_1,\ L_2$ have a form

$$L_1 = \frac{d^4}{dr^4} + \frac{2}{r}\frac{d^3}{dr^3} - \frac{3}{r^2}\frac{d^2}{dr^2} + \left(\frac{3}{r^3} + 2in^3\right)\frac{d}{dr} + \left(-\frac{3}{r^4} + n^4\right)$$

$$L_2 = \frac{d^2}{dr^2} + \frac{1}{r}\frac{d}{dr} - \left(\frac{1}{r^2} - n^2\right) = 0.$$

In paper [29] we showed that the first terms of the asymptotic expansion in zero of eigenfunctions of the problem (46), (48), (49), (50), (51) are a linear combination

$$u_0 = \alpha r + \beta r^3.$$

Hence, operators $L_3,\ L_4$ are defined as:

$$L_3 = r^2\frac{d^2}{dr^2} - 3r\frac{d}{dr} + 3, \qquad L_4 = 0.$$

We discretize both equations taking into account the right boundary condition and get matrix beams

$$A_1 - \mu B_1 = L_1(\mathrm{diag}(r_j), D_{00}) - \mu L_2(\mathrm{diag}(r_j), D_{00}),$$
$$A_0 - \mu B_0 = L_3(\mathrm{diag}(r_j), D_{00}) - \mu L_4(\mathrm{diag}(r_j), D_{00}).$$

If vector $\mathbf{u} = (u_1, \dots, u_{N-1})^T$, $u_j = u(r_j)$, approximates eigenfunction $u(r)$, then the vector correlation $(A_1 - \mu B_1)\mathbf{u} = 0$ holds for every component (i.e. everywhere in $[0, 1]$). And from correlations $(A_0 - \mu B_0)\mathbf{u} = 0$ only the first (i.e. near zero) is approximately fulfilled. We glue these beams as follows:

$$A^{\mathrm{as}} = \begin{pmatrix} \bar{A}_0 \\ \underline{A}_1 \end{pmatrix}, \qquad B^{\mathrm{as}} = \begin{pmatrix} \bar{B}_0 \\ \underline{B}_1 \end{pmatrix},$$

where $\bar{A}_0, \bar{B}_0$ are first rows of matrices A_0, B_0, $\underline{A}_1, \underline{B}_1$ are rows of matrices A_1, B_1, starting from the second and ending with the last. After that we solve an algebraic spectral problem for the matrix beam $A^{\mathrm{as}} - \mu B^{\mathrm{as}}$.

Thus to solve the spectral problem we can either use its original form as a system or transform it to a high-order equation. Both approaches have their advantages and disadvantages. The discretization of systems leads to matrix beams of large sizes where the matrix for spectral parameter is always singular. It means that the matrix beam has infinite eigenvalues which on one side makes the discrete operator even more similar to the differential

one which also has a series of eigenvalues converging to infinity. But due to computational errors instead of infinite eigenvalues we get ones with a large module which leads to a "cloud" surrounding the infinite point. This gives us a criterion to exclude such eigenvalues from further consideration. Besides with an unlucky use of collocation matrix derivatives we can even get singular matrix beams which should be avoided. However the norms of matrix beams remain rather small which allows for more accurate calculation of eigenvalues.

The norms of matrices we get after the discretization of equations can be rather large when using a fine computational grid which lowers the accuracy of calculating eigenvalues. As an advantage we can note that transforming the system into equation excludes the variable connected to pressure and anisotropy tensor which in turn eliminates the dependence of the decision on the choice of boundary conditions for these functions.

Here is a short description of the approach used to separate "true" eigenvalues from "parasitic" ones. The calculations were done for three dimensions $N_1 < N_2 < N_3$. After that for each eigenfunction $v_j^{[N_1]}$ we find eigenfunctions closest to it

$$v_j^{[N_1]} \approx v_j^{[N_2]} \approx v_j^{[N_3]}, \qquad j = 1, \ldots, N_1.$$

For that we interpolate eigenfunctions for dimensions N_2, N_3 on the grid for the dimension N_1 and compare them to each other in the nodes of the grid. Based on the correspondence between eigenfunctions we get the correspondence between spectrum points $\lambda_j^{[N_1]} \approx \lambda_j^{[N_2]} \approx \lambda_j^{[N_3]}$.

Then we calculate values of a number of criterions. Among them are: proximity of corresponding eigenvalues

$$|\lambda_j^{[N_1]} - \lambda_j^{[N_2]}|, \quad |\lambda_j^{[N_2]} - \lambda_j^{[N_3]}|;$$

proximity of corresponding eigenfunctions

$$\|v_j^{[N_1]} - v_j^{[N_2]}\|, \quad \|v_j^{[N_2]} - v_j^{[N_3]}\|,$$

where we can use both Euclidean norm and maximum absolute value as a norm; the variation of eigenfunctions

$$\operatorname{var} v_j^{[N_1]}, \quad \operatorname{var} v_j^{[N_2]}, \quad \operatorname{var} v_j^{[N_3]},$$

defined for example as

$$\operatorname{var} v^{[N_1]} = \sum_{k=1}^{N-1} |v_{k+1} - v_k|.$$

Values of each of the criterions or their combination is sorted in ascending order. We then calculate the maximal relative difference between the sorted neighboring criterions, i.e. "jump". This "jump" delimits eigenvalues that we consider "true" from the ones we stop considering. Thus we eliminate points that do not converge for either eigenvalues or eigenfunctions or which

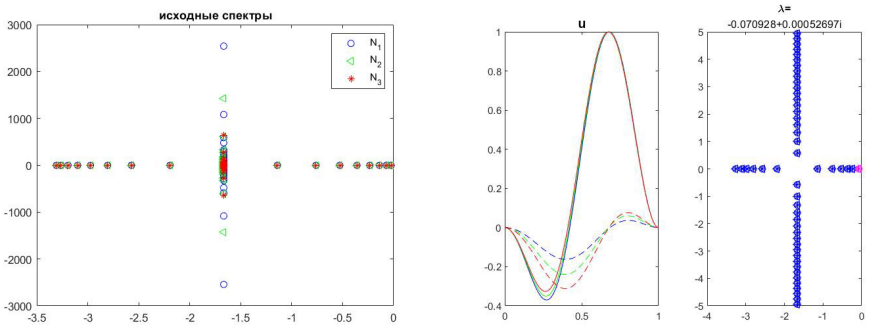

FIGURE 2. Spectrum of the problem (47), (52), (53) before the use of criterions (left). Eigenfunction for the rightmost eigenvalue and spectrum after the use of criterions (right). Colour highlights the rightmost eigenvalue.

eigenfunctions have s distinct saw-like structure. Numerical results and their analysis is given in the next part.

4 Results of numerical experiments

First of all note that as stated above to find pairings of eigenvalues to eigenfunctions that doesn't change with the growth of grid nodes count we use three values of N. For further examples these values are $N_1 = 100$, $N_2 = 150$, $N_3 = 200$. For graphs of eigenfunctions for different values of N, we use the following colours: blue is for N_1, green is for N_2, red is for N_3, the solid line is for the real part of the function, the dashed line is for the imaginary part of the function. For the spectrum points circles correspond to N_1, triangles to N_2, stars to N_3.

Let **Re=500, Wi=0.3, n=1**.

The left part of fig. 2 illustrates the way the calculated spectrum changes with the use of criterions for eigenvalues. In the right part of graphs of fig. 2 we can see that for the problem (47), (52), (53) there is a weak convergence of eigenvalues and eigenfunctions. Note that the situation is similar for the problem (45), (52), (53) (see fig. 3).

The results of computations for the problem (44),(48), (50) without the additional condition (54) and with it are presented in fig. 4. We can see that the additional condition doesn't change the result. But the existence of the condition simplifies the construction of the discrete operator by allowing us to use the same grids and the same sized collocation matrix derivatives for all three unknown functions.

Fig. 5 shows results of computations for equation (46) with conditions (48), (50). Here we use two methods of mapping boundedness conditions to the structure of matrix derivatives. We also see a pronounced consistency of results among themselves.

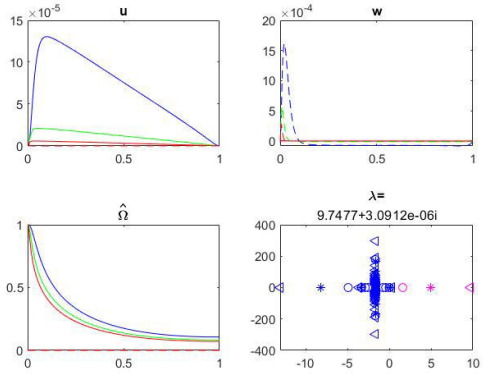

FIGURE 3. Eigenfunction for the rightmost eigenvalue and spectrum after the use of criterions (right) for the problem (45), (52), (53).

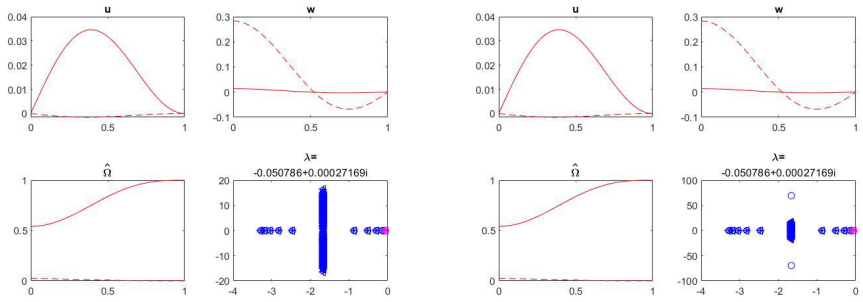

FIGURE 4. Components of the eigenfunction for the rightmost eigenvalue and spectrum after the use of criterions for the system (44) with conditions (48), (50) without the condition on the function $\hat{\Omega}$ (left) and with additional conditions (54) (right).

Note that the rightmost eigenvalues for the system and for the equation are in the left half-plane but their values differ. Corresponding eigenfunctions exhibit similar behaviour but have some difference in imaginary parts.

Let **Re=500, Wi=0.3, n=10**.

With the growth of parameter n the rightmost eigenvalues move to the right half-plane. Fig. 6 shows the situation where for the system this value is still in the left half-plane but for the equation is already in the right half-plane. Also note that the components u of corresponding eigenfunctions for the equation and for the system are significantly different. The overall structure of the spectrum for the equation and for the system also differs.

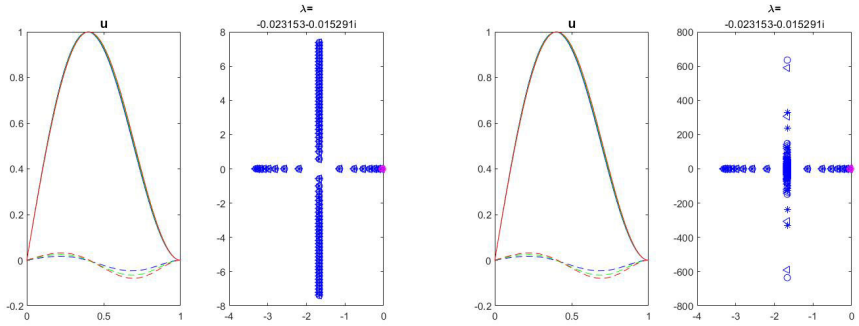

FIGURE 5. Eigenfunction for the rightmost eigenvalue and spectrum after the use of criterions for the problem (46), (48), (50). To the left boundary conditions are discretized using the function multiplication method, to the right boundary conditions are discretized using the asymptotic method.

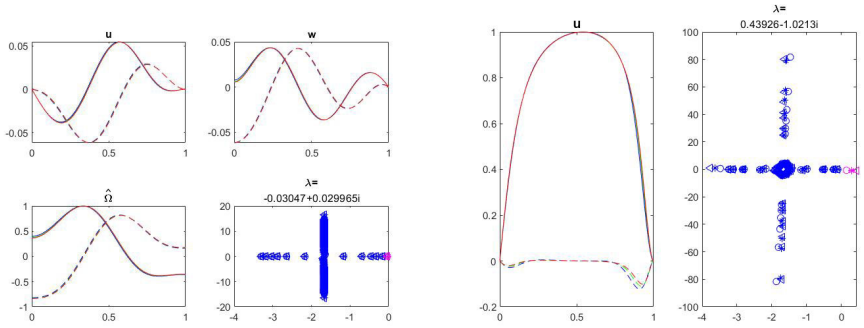

FIGURE 6. Components of the eigenfunction for the rightmost eigenvalue for the system (44) (left) and the equation (46) (right) with conditions (48), (50).

Let **Re=500, Wi=0.3, n=20**.

For these parameters both the system and the equation have one eigenvalue in the right half-plane. The difference in spectrum structure and in eigenfunction keeps growing (fig. 7).

Finally let **Re=500, Wi=0.3, n=50**.

For these parameters one eigenvalue is again in the right half-plane. Note that the eigenvalue for the equation is situated significantly further to the right than the eigenvalue for the system. Their imaginary parts also differ. Also of note is the fact that convergence process for the equation eigenvalue is still ongoing despite rather large values of N. The general spectrum structure and eigenfunctions keep being significantly different (fig. 8).

Since the most important question for us is the question of stability we study the behaviour of a number of eigenvalues with the largest real part

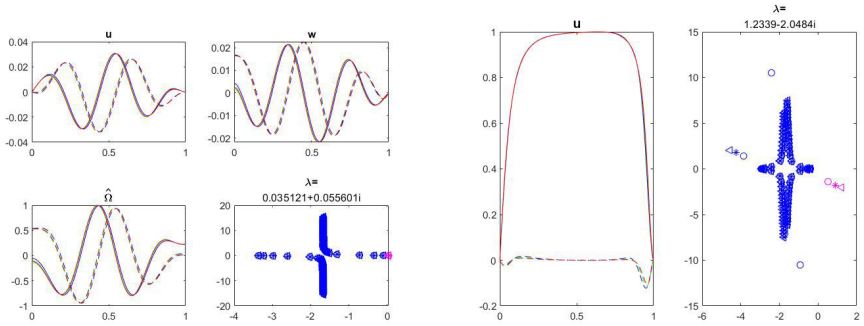

FIGURE 7. Components of the eigenfunction for the rightmost eigenvalue for the system (44) (left) and the equation (46) (right) with conditions (48), (50).

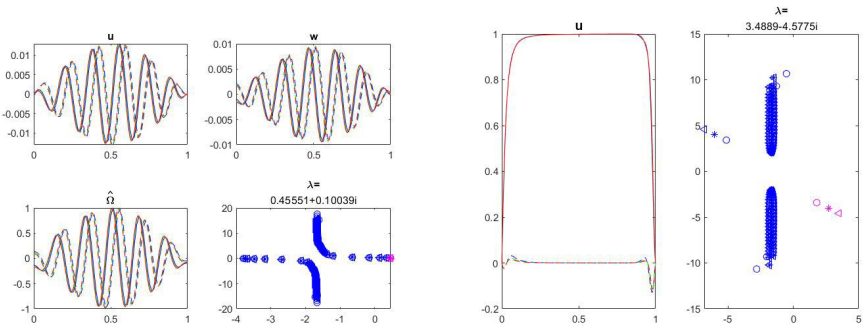

FIGURE 8. Components of the eigenfunction for the rightmost eigenvalue for the system (44) (left) and the equation (46) (right) with conditions (48), (50).

and its dependences of n. Further we assume that eigenvalues are numbered right to left, i.e. the rightmost eigenvalue has the number 1. Below we study the behaviour of λ_1, λ_2, λ_3.

To start we consider the problem (46), (48), (49), (50), (51), discretized by using the information about asymptotic behaviour near zero which was presented earlier in [29]. However here we use different approaches and the study itself is much deeper.

We construct graphs that show the dependence of the real part of λ_j, $j = 1, 2, 3$, on n for $N_1 = 100, N_2 = 150, N_3 = 200$ and different values of Weissenberg and Reynolds numbers (fig. 9).

Take note of some significant moments. The rightmost eigenvalue (blue colour) demonstrates weak convergence by N or even no convergence for relatively large n. To have this value shown on graphs we had to turn off automatic filtration of the computed spectrum by the criterion of the convergence of eigenvalues. But even without it the filtering by eigenfunctions

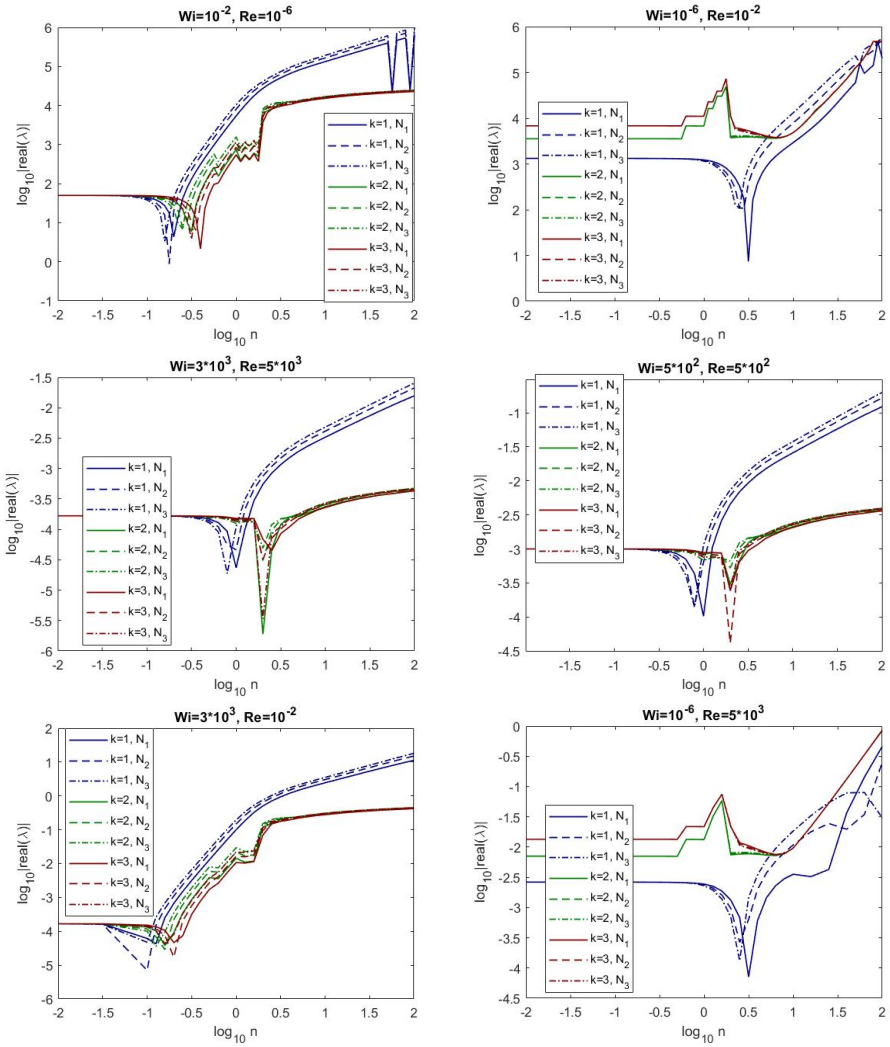

FIGURE 9. Graphs of real parts of eigenvalues for the problem (46), (48), (49), (50), (51), discretized by asymptotic method.

also sometimes leads to excluding this eigenvalues from the set of "true" ones and then blue graphs "collapse" with graphs of other eigenvalues (see fig. 9, two upper graphs).

In every example shown so far for small values of n the spectrum alway lies in the left half-plane.

For most graphs represented in fig. 9 eigenvalues $\lambda_1, \lambda_2, \lambda_3$ go into the right half-plane in order with the growth of n. The transition through the imaginary axis happens when graphs form an edge pointed down, i.e. logarithm goes to $-\infty$. After its transition the value λ_1 continues to move away from the imaginary axis while values of λ_2, λ_3 either stabilizes on a certain

distance or move away much slower (see fig. 9, left vertical row and middle horizontal raw).

If the Weissenberg number is significantly smaller than the Reynolds number (upper and lower right graphs) then there is only one eigenvalue that goes to the right half-plane. Morever interestingly for large values of Reynolds eigenvalue λ_1 comes back to the left half-plane (lower right graph). For different values of N it happens for significantly different values of n.

Now we want to check how much difference the way we take into account left boundary condition creates in properties of the spectrum (46), (48), (49), (50), (51). We discretize it using the function multiplication method. The spectrum of a problem discretized in this way contains four horizontal branches directed to the right and to the left. With the growth of N these branches move significantly while containing eigenvalues corresponding to the high-frequency eigenfunctions. This means that these branches are "artifacts" of discretization. Automatic filtration of the spectrum we are making allows to throw away these eigenvalues. However there is a high probability of also throwing away the rightmost eigenvalue. It can be seen on all graphs from fig. 10, where for $n > 10$ graphs for λ_1 are exactly like graphs for λ_2, λ_3. Aside from this feature all graphs from fig. 10 are very similar to graphs from fig. 9.

Now we consider the problem (44), (48), (50), discretized using the function multiplication method. On fig. 11 we can see the location of three rightmost eigenvalues of the system. The fact that there is a good convergence by N attracts attention: curves corresponding to $N_1 = 100, N_2 = 150, N_3 = 200$ merge completely. All three of considered eigenvalues for some values of n transit from the left half-plane to the right one and then continue to move away from the imaginary axis with the growth of n. The transition happens even for those values of Wi and Re, that for equation resulted in only one eigenvalue being in the right half-plane but for significantly larger n. If we continue the comparison to eigenvalues of the equation we can notice the following: the growth of the real part of the system eigenvalues is less than the growth of the real part of the first eigenvalue of the equation but more than the growth of the real part of the second and third eigenvalues of the equation.

5 Conclusion

In the computational part of this work we carried out a numerical study of spectral problems. We used different variants of the mathematical statement of the problem and different ways of discretization. It turns out that the use of different boundary conditions on $\hat{\Omega}$ does not influence the numerical result but significantly simplifies working with the discrete differential operator.

All approaches demonstrate that for small n all spectrum is in the left half-plane but with the growth of n one or several eigenvalues transit to the right half-plane.

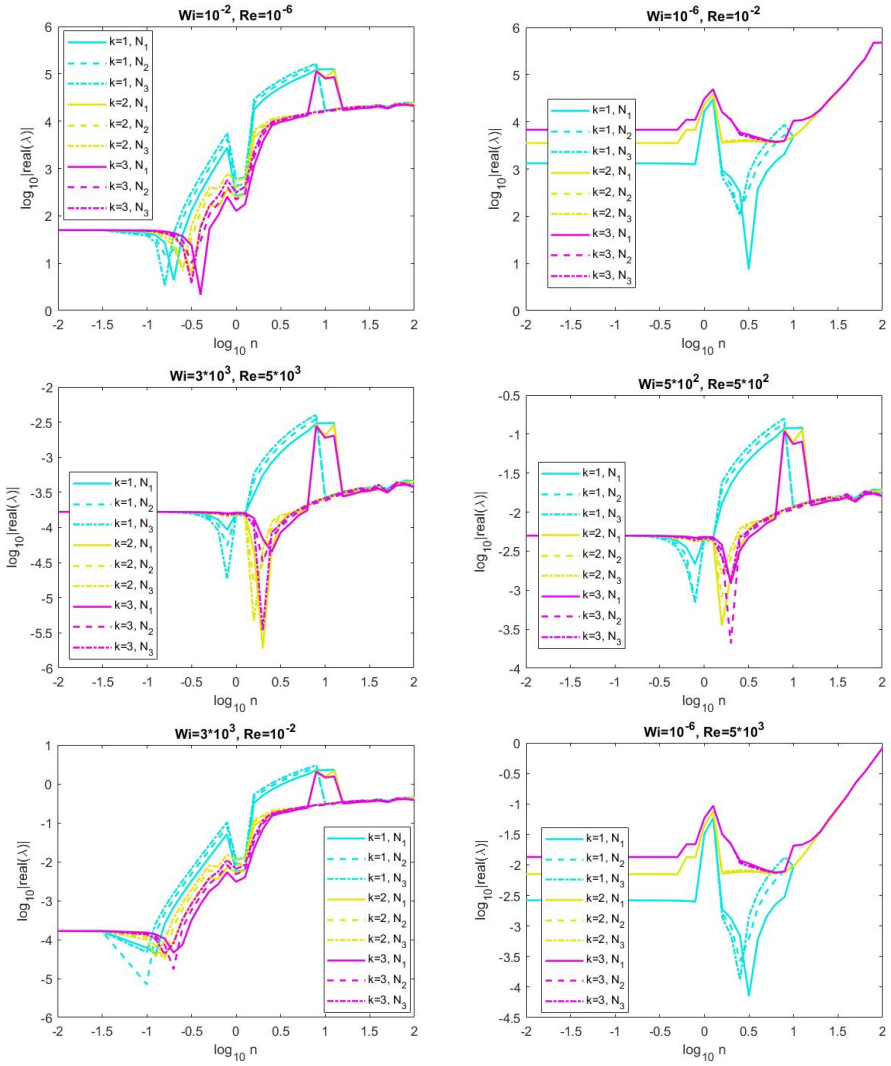

FIGURE 10. Graphs of real part of eigenvalues for the problem (46), (48), (49), (50), (51), discretized by function multiplication method.

We establish that two different ways of taking into account boundary conditions during discretization (asymptotic method and function multiplication method) give identical results. At the same time the critical i.e. the rightmost eigenvalue converges weakly if at all for large values of n so its connection to the spectrum of the original differential operator is rather dubious.

On the other hand the spectrum we calculated for the system converges well and behaves in a predictable way. However the most unexpected are results pointing to the difference between spectrums acquired for the discrete

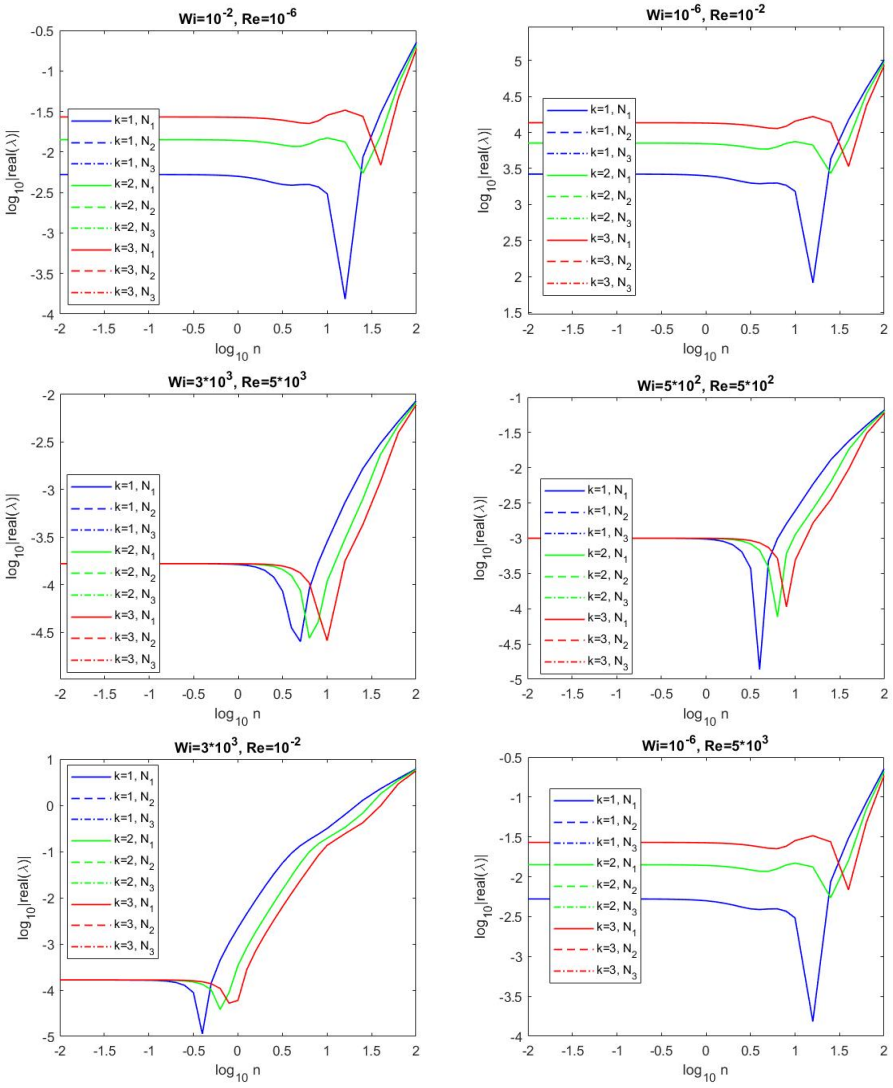

FIGURE 11. Graphs of real part of eigenvalues for the problem (44), (48), (50), discretized by function multiplication method.

system and the discrete equation derived from it. But noticing that the spectrum of the system is computed more accurately with the growth of N and converges better means that this approach is preferable. The reasons for such significant difference require additional research.

References

[1] V.N. Pokrovskii, *The mesoscopic theory of polymer dynamics*, 2nd Ed., Springer, London, 2010.

[2] Yu.A. Altukhov, A.S. Gusev, G.V. Pishnograi, *Introduction into mesoscopic theory of flowing polymeric systems*, Alt. GPA, Barnaul, 2012. (in Russian)

[3] J.G. Oldroyd, *On the formulation of rheological equations of state*, Proc. R. Soc., Ser. A. **200** (1950), 523–541. Zbl 1157.76305

[4] R.B. Bird, P.J. Dotson, N.L. Johnson, *Polymer solution rheology based on a finitely extensible bead-spring chain model*, J. Non-Newtonian Fluid Mech., **7** (1980), 213–235. Zbl 0432.76012

[5] M.D. Chilcott, J.M. Ralliston, *Creeping flow of dilute polymer solutions past cylinders and spheres*, J. Non-Newtonian Fluid Mech., **29**:3 (1988), 381–432. Zbl 0669.76016

[6] J. Remmelgas, G. Harrison, L.G. Leal, *A differential constitutive equation for entangled polymer solutions*, J. Non-Newtonian Fluid Mech., **80**:2 (1999), 115–134. Zbl 0951.76005

[7] V.N. Polrovski, *Statistical mechanics of dilute suspension*, Nauka, Moscow, 1978 (in Russian).

[8] S.A. Zinovich, I. E. Golovicheva, G.V. Pyshnograi, *Influence of the molecular mass on the shear and longitudinal viscosity of linear polymers*, Prikl. Mekh. Tekh. Fiz., **41**:2 (2000), 154–160. (in Russian). Zbl 0999.74032

[9] G. Pyshnograi, D. Merzlikina, P. Filip, R. Pivokonsky, *Mesoscopic single and multimode rheological models for polymeric melts viscometric flow description*, WSEAS transactions on heat and mass transfer, **13** (2018), 49–65.

[10] A.M. Blokhin, D.L. Tkachev, *Linear asymptotic instability of a stationary flow of a polymeric medium in a plane channel in the case of periodic perturbations*, J. Appl. Ind. Math. **8**:4 (2014), 467–478. Zbl 1340.76037

[11] A.M. Blokhin, A.V. Yegitov, D.L. Tkachev, *Linear instability of solutions in a mathematical model describing polymer flows in an infinite channel*, Comput. Math. Math. Phys., **55**:5 (2015), 848–873. Zbl 1426.76153

[12] A.M. Blokhin, D.L. Tkachev, *Spectral asymptotics of a linearized problem about flow of an incompressible polymeric fluid. Base flow is analogue of a Poiseuille flow*, AIP Conf. Proc., **2027** (2018), 030028.

[13] A.M. Blokhin, D.L. Tkachev, *Analogue of the Poiseuille flow for incompressible polymeric fluid with volume charge. Asymptotics of the linearized problem spectrum*, J. Phys. Conf. Ser., **894**:012096 (2017), 1–6.

[14] A.M. Blokhin, A.V. Yegitov, D.L. Tkachev, *Asymptotics of the spectrum of a linearized problem of the stability of a stationary flow of an incompressible polymer fluid with a space charge*, Comput. Math. Math. Phys., **58**:1 (2018), 102–117.

[15] A. Blokhin, D. Tkachev, A. Yegitov, *Spectral asymptotics of a linearized problem for an incompressible weakly conducting polymeric fluid*, Z. Angew. Math. Mech., **98**:4 (2018), 589–601. Zbl 7776847

[16] A.M. Blokhin, D.L. Tkachev, *Stability of Poiseuille-type flows for an MHD model of an incompressible polymeric fluid*, J. Hyperbolic Differ. Equ., **16**:4 (2019), 793–817. Zbl 1442.76136

[17] A.M. Blokhin, D.L. Tkachev, *Stability of the Poiseuille-type flow for a MHD model of an incompressible polymeric fluid*, Eur. J. Mech. B. Fluids **80** (2020), 112–121. Zbl 1436.76061

[18] A.M. Blokhin D.L. Tkachev, *Stability of Poiseuille-type flows for an MHD model of an incompressible polymeric fluid*, Fluid Dyn., **54**:8 (2019), 1051–1058. Zbl 1457.76072

[19] A.M. Blokhin, D.L. Tkachev, *Stability of Poiseuille-type flows in an MHD model of an incompressible polymeric fluid*, Sb. Math., **211**:7 (2020), 901–921. Zbl 1450.76009
[20] V.S. Vladimirov, *Generalized functions in mathematical physics*, Moscow, Nauka, 1979 (in Russian). Zbl 0515.46033
[21] L. Hórmander, *The analysis of linear partial differential operators. I: Distribution theory and Fourier analysis*. Springer-Verlag, 1983. Zbl 0521.35001
[22] A.M. Blokhin, D.L. Tkachev, *MHD model of incompressible polymeric fluid. Linear instability of the resting state*, Complex Var. Elliptic Equ., **66**:6-7 (2021), 929–944. Zbl 1466.76023
[23] A.M. Blokhin, D. Tkachev, *Linear instability of the resting state for the MHD model of an incompressible polymeric fluid*, AIP Conf. Proc., **2351**:1 (2021), 040057.
[24] A.M. Blokhin, D.L. Tkachev, *On Linearly Unstable Steady States of an MHD Model of an Incompressible Polymeric Fluid in the Case of Absolute Conductivity*, Sib. Adv. Math., **32** (2022), 1–12.
[25] A.M. Blokhin, A.Yu. Goldin, *Linear Stability of an Incompressible Polymer Fluid at Rest*, J. Math. Sci., **230**:1 (2018), 14–24.
[26] D.L. Tkachev, *Spectrum and linear Lyapunov instability of a resting state for flows of an incompressible polymeric fluid*, J. Math. Anal. Appl., **522** (2023), 126914. Zbl 1523.76039
[27] D.L. Tkachev, *The spectrum and Lyapunov linear instability of the stationary state for polymer fluid flows: the Vinogradov-Pokrovskii model*, Sib. Math. J., **64**:2 (2023), 407–423. Zbl 1511.76029
[28] G.I. Taylor, *Stability of a Viscous Liquid contained between Two Rotating Cylinders*, Lond. Phil. Trans. (A), **223**:289–343 (1923). Zbl 49.0607.01
[29] D.L.Tkachev, E.A. Biberdorf, *Spectrum of a problem about the flow of a polymeric viscoelastic fluid in a cylindrical channel (Vinogradov- Pokrovski model)*, Sib. Èlektron. Mat. Izv., **20**:2 (2023), 1269–1289. Zbl 1547.35575
[30] A.M. Blokhin, A.S. Rudometova, *Stationary flows of a weakly conducting incompressible polymeric liquid between coaxial cylinders*, Journal of Applied and Industrial Mathematics, **11**:4 (2017), 486-493.
[31] A.M. Blokhin, R.E. Semenko, A.S. Rudometova, *Magnetohydrodynamic Vortex Motion of an Incompressible Polymeric Fluid*, J. Appl. Ind. Math., **15**:1, 7–16. Zbl 1511.76114
[32] D.L.Tkachev, E.A. Biberdorf, *Spectrum of a linear problem about the MHD flows of a polymeric fluid in a cylindrical channel in case of an absolute conductivity (Generalized Vinogradov-Pokrovski model)*, Sib. Èlektron. Mat. Izv., **21**:2 (2024), 823–851.
[33] D.L. Tkachev, A.V. Yegitov, E.A. Biberdorf, *Linear instability of a resting state of the magnetohydrodynamic flows of polymeric fluid in a cylindrical channel (generalized Vinogradov–Pokrovski model)*, Physics of Fluids, **36**:9 (2024), 093115.
[34] B.V. Semisalov, I.A. Bugoets, L.I. Kutkin, *Simulation of the non-stationary non-isothermal polymer fluid flow through the channel with elliptic cross-section*, Sib. Èlektron. Mat. Izv., **22**:1 (2025), 252–273 (in Russian).
[35] M. Abramowitz, I. Stegun, *Handbook of Mathematical Functions*, NBS, 1964. Zbl 0171.38503
[36] L.I. Sedov, *Mechanics of Continuous Medium. Vol. 1*, Moscow, Nauka, 1970. (in Russian)
[37] L.G. Loytsyanskiy, *Mechanics of Fluids and Gas*, Moscow, Nauka, 1978. (in Russian)
[38] Shih-I Pai, *Introduction to the Theory of Compressible Flow*, New York, D. Van Nostrand, 1959. Zbl 0091.18004
[39] L.N. Trefethen, *Spectral Methods in MATLAB*, SIAM, Philadelphia, 2000.

[40] S.K. Godunov, V.T. Zhukov, O.B. Feodoritova, *A method for calculating invariant subspaces of symmetric hyperbolic equations*, Comput. Math. Math. Phys., **46**:6 (2006), 971–982. Zbl 1549.35304

Dmitry Leonidovich Tkachev
Sobolev Institute of Mathematics,
pr. Koptyuga, 4,
630090, Novosibirsk, Russia
Email address: tkachev@math.nsc.ru

Elina Arnoldovna Biberdorf
Sobolev Institute of Mathematics,
pr. Koptyuga, 4,
630090, Novosibirsk, Russia
Email address: ermolova@math.nsc.ru